Journal of Photochemistry and Photobiology A: Chemistry 201 (2009) 222–227

Contents lists available at ScienceDirect

Journal of Photochemistry and Photobiology A: Chemistry

journal homepage: www.elsevier.com/locate/jphotochem

The influence of photosensitizers on the photorefractivity in poly[methyl-3-(9-carbazolyl)propylsiloxane]-based composites

Jin-Woo Oh[a], In Kyu Moon[b], Nakjoong Kim[a,*]

[a] Department of Chemistry, Hanyang University, 17 Haengdang-Dong, Seongdong-Gu, Seoul 133-791, Republic of Korea
[b] Environment and Energy Division, Korea Institute of Industrial Technology, 35-3 Hongcheon, Cheonansi, Chungnam 330-825, Republic of Korea

ARTICLE INFO

Article history:
Received 27 March 2008
Received in revised form 28 October 2008
Accepted 4 November 2008
Available online 12 November 2008

Keywords:
Photosensitizer
Photo-charge generation
Photocurrent
Space charge field
PR grating buildup time

ABSTRACT

We investigated the photosensitizers effect on the photorefractive (PR) properties in five poly[methyl-3-(9-carbazolyl)propylsiloxane] (PSX-Cz)-based PR composites which were doped with various photosensitizers having each different electron affinity, such as 2,4,5,7-tetranitro-9H-fluorine-9yilden malonitrile (TeNFM), 2,4,7-trinitro-9-fluorenone (TNF), 9-dicyanomethylene-2,4,7-trinitro-fluorenone (TNFM), tetracyanoethylene (TCNE), and 7,7,8,8-tetracyanoquinnodimethane (TCNQ). At 632.8 nm, photo-charge generation efficiencies, photoconductivities, space charge field, four wave mixing diffraction efficiencies, and PR grating buildup times were measured as a function of external electric field. The photo-charge generation, which is dependent on the light absorption, was achieved through the charge transfer (CT) complexes between the PSX-Cz and each of the photosensitizers. The photon energy of the CT transition decreased with increasing electron affinity of the photosensitizer. In composites doped with TeNFM, TNF, and TNFM, the space charge field (E_{sc}) increased as the photo-charge generation efficiency increased; the grating buildup in these composites is rate-limited by the photo-charge generation speed. In sample doped with TCNE, and TCNQ, the hole mobility was reduced due to the larger amount of photosensitizer anion traps produced by photoreduction of the photosensitizer. Then, the grating buildup speed became hole mobility limited, and smaller buildup rates were observed. The magnitude of space charge field was sustained as the charge and trap density increased. In all composites, the refractive index modulation is increased with the magnitude of space charge field.

1. Introduction

The photorefractive (PR) effect based on both the electro-optic effect and the space charge field formation can be demonstrated in various organic and inorganic materials such as $BaTiO_3$, $LiNbO_3$, and carbazole based polymeric systems [1–3]. Compared to inorganic crystals, the polymeric systems have a great disadvantage in that they require an electric field far above 10 V/μm for transporting electric carriers to form the E_{sc} within polymeric system. Nevertheless, the reasons why the polymeric systems have received a great deal of attention for a long time are the advantages of excellent PR performance, low cost and high processability that allows for manufacturing various shaped devices. In addition, PR performance can be readily controlled by changing composition of polymeric system [4].

During the last decades, using the PR effect, various potential applications have been demonstrated in holographic data storage and information processes such as pattern recognition, phase conjugation mirror, and optically controlled spatial light modulator [5–7]. And, it can be used in biomedical application of optical coherent tomography of thick biological tissues [8]. However, until now, no PR system satisfied all specifications necessary for commercialization. In particular, the slow hologram recording/erasing speed, PR performance reliabilities, and the low optical sensitivity are considered the most serious problems. In the holographic information processing, the fast processing speed is the most important specification rather than others. On the other hand, as the biomedical tomography, high optical sensitivity becomes more important for obtaining distinct information from the weak optical signals scattered from objects such as tissues. It needs a breakthrough in these two factors, high speed in recording and high optical sensitivity for the commercialization of polymeric PR systems. For the breakthrough, it is important to find key factors determining specific PR performance, which can be achieved from the accumulation of basic research on each composite that compose the polymeric PR system.

* Corresponding author. Tel.: +82 2 2220 0935; fax: +82 2 2295 0572.
E-mail address: kimnj@hanyang.ac.kr (N. Kim).

1010-6030/$ – see front matter © 2008 Elsevier B.V. All rights reserved.
doi:10.1016/j.jphotochem.2008.11.001

Both the speed and the sensitivity issues are closely related with the E_{sc} formation [9]. It is desirable that the E_{sc} is generated with the faster speed and by the lower light intensity rather than current levels. The E_{sc} is formed through the following processes: the photo-charge generation, the transport and the trap of the generated charges [10]. The photo-charge generation depends on the CT behavior between a photosensitizer and a photoconducting polymer. The interaction between the photoconducting polymer and the photosensitizer leads to a new absorption band that does not appear in the spectrum of either component alone. Hence spectral sensitivity in the visible and the near infrared part of the spectrum can be achieved with CT complexes [11]. The CT complex can be separated into electrons and holes by the electron–hole separation distance in the excited state and the magnitude of the electric field that is applied over the PR composite. After separation of the CT complex into electrons and holes, the holes can hop from one site to another in the photoconducting polymer with the aid of a strong electric field [12]. As a result of the trapping process, the trapped charges form a spatially varying space charge field. Although the trap of charges is very important in the space charge formation [13], it is difficult to consider it a control parameter. Therefore, the photoconducting polymer and the photosensitizer must be key factors for determining the properties of the E_{sc}.

In this work, photosensitizer effect on the overall PR properties was investigated from the CT behavior to PR performance in order to evaluate the importance of the photosensitizer in polymeric PR composite. First, the charge transfer complexes between the photoconducting polymer and different photosensitizers were examined through UV absorption spectrum, photo-charge generation efficiency and photoconductivity. Then, on the basis of these results, we discussed the relation between the photosensitizer and the PR performances such as magnitude of space charge field, modulation of the refractive index and PR grating buildup time. Experimentally, host photoconducting polymer and nonlinear optical (NLO) chromophore were fixed and only photosensitizer was varied for preparing the test composites.

2. Experimental

2.1. Materials and instrumentation

Photorefractive composite was prepared by blending of photoconducting polymer matrix, photosensitizer and NLO chromophore in the ratio of 79:1:20 by wt%, respectively. The photoconducting polymer matrix, poly[methyl-3-(9-carbazolyl)propylsiloxane] (PSX-Cz) and the NLO chromophore, 2-{3-[(*E*)-2-(dibutylamino)-1-ethenyl]-5,5-dimethyl-2-cyclohexenyliden}malono-nitrile (DB-IP-DC) were chosen and fixed, because they are chemically stable, plus their chemical and physical properties have been well known in literature [14]. In the PR composite preparation, we used five different photosensitizers; 2,4,5,7-tetranitro-9H-fluorine-9yilden malonitrile (TeNFM), 2,4,7-trinitro-9-fluorenone (TNF), 9-dicyanomethylene-2,4,7-trinitro-fluorenone (TNFM), 7,7,8,8-tetracyanoquinnodimethane (TCNQ) and tetracyanoethylene (TCNE), to provide photosensitivity in the 632.8 nm. Fig. 1 shows the chemical structures of the materials used in this study. PSX-Cz and DB-IP-DC were synthesized using previously described methods [15]. These photosensitizers were obtained from Kanto Chemistry Co. and were used after purification by using the sublimation method.

The glass transition temperature (T_g) of the PR composites was determined by differential scanning calorimetry (PerkinElmer DSC7) at a heating rate of 10 °C/min. The polymeric PR composites containing 20 wt% of the DB-IP-DC chromophore showed a T_g in the range of 26–32 °C without the addition of extra plasticizer.

2.2. Sample preparation and measurement

For the PR device fabrication, the mixture (total 100 mg) was dissolved in 400 ml of dichloromethane and the solution was filtered through a 0.2 μm membrane. The PR composite was cast on a patterned indium tin oxide (ITO) glass substrate, dried slowly for 6 h at ambient temperature, and then heated in an oven to 90 °C for 24 h to completely remove the residual solvent. The composite

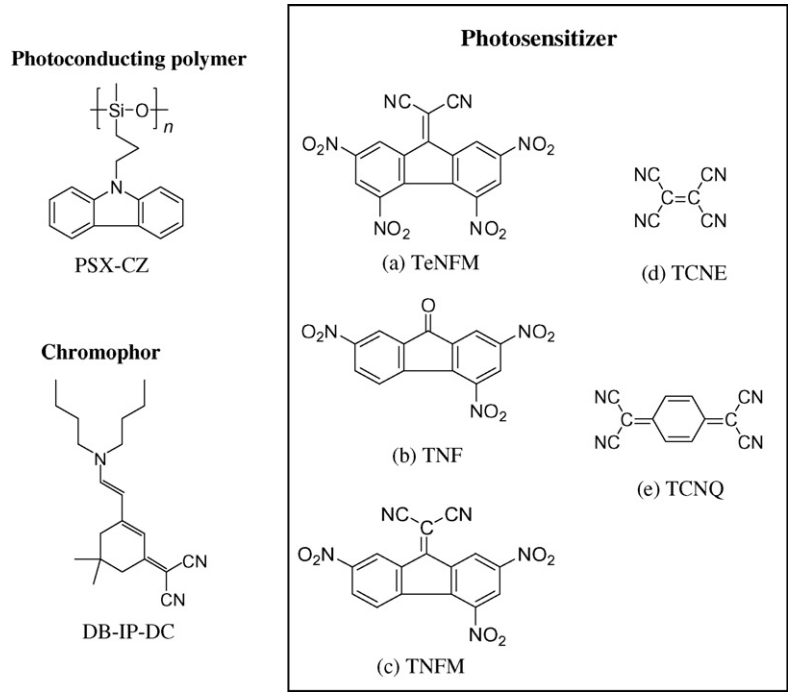

Fig. 1. Chemical structures of the components for the photorefractive composites: photoconducting polymer matrix, chromophore, and photosensitizers.

Table 1
Photosensitizer type, electron affinity (EA) of the photosensitizer, molecular weight (MW) of the photosensitizer, number of the photosensitizer molecule (mol), absorption coefficient (α), photo-charge generation efficiency (Φ), photoconductivity (σ), grating buildup time (τ), and glass transition temperature (T_g) in composites 1–5.

#	Photo-sensitizer	EA (eV)	MW	mol (10^{-6})	α (cm^{-1})[b]	Φ (10^{-4})[a,b]	σ (pS/cm)[a,b]	τ (s)[a,b]	T_g (°C)
1	TeNFM	2.56	408	2.45	18.0	0.70	1.47	1.95	30.7
2	TNF	2.17	315	3.17	20.5	1.25	2.99	0.49	32.3
3	TNFM	2.42	363	2.75	32.1	1.85	3.52	0.26	29.7
4	TCNE	2.77	128	7.81	35.7	1.89	0.45	5.97	26.8
5	TCNQ	2.84	204	4.90	39.5	2.20	1.09	2.68	26.2

[a] Measured at $E_0 = 60\,V/\mu m$.
[b] Measured at $\lambda = 632.8\,nm$.

was then softened on a hot plate at 100 °C, and next sandwiched between ITO glasses with Teflon film spacer of 80 μm to yield a film with a uniform thickness [14]. The thickness of the active layer was near 80 μm.

Since optical nonlinearity of our PR composites is based on the alignment of the rod-like chromophores towards electric field within the composite, it should be sensitive to the measurement temperature, especially the temperature difference with the near T_g of the composites. The measurement temperature of the PR devices was carefully controlled with a device holder designed in our laboratory which can be adjusted from 20 to 50 °C with error range of ±0.2 °C. There was a 1.5 cm diameter hole at the center of the heating plate of the composite holder. The laser beams illuminating the composite passed though through this hole. The composite temperature was monitored using a thermometer (Fluke 50S), whose probe was placed in contact with the glass plate of the composite.

The photo-charge generation efficiencies of the composites were determined by using the xerographic discharge technique [15,16]. Under emission-limited conditions, the photo-charge generation efficiency was independent of the carrier drift velocity and was determined only by the generation rate of free carriers [17]. For the photogeneration efficiencies measuring, polymer mixtures (PSX-Cz:DB-IP-DC:photosensitizer = 79:20:1 wt%) are dissolved in a 1,1,2,2-tetra chloroethane and the films are fabricated by doctor-blade technique onto a 2.5 cm × 2.5 cm ITO glass substrate. Layer thickness (~3.5 μm) is measured by using the Metricon. The photo-charge generation efficiencies of composites were calculated from the amplitude of the photovoltage measured by electrometer (TREK model 344) under the wavelength of 632.8 nm light ($I = 3.6\,mW/cm^2$) which is 1 cm in diameter.

The photoconductivities of the composites were measured at a wavelength of 632.8 nm using a simple dc photocurrent method. The current flowing through the composite was measured using the Keithley 6485 during illumination with an intensity of 20 mW/cm^2 at an applied field of 60 V/μm [18].

The diffraction efficiency of the PR materials was determined using a degenerate four wave mixing (DFWM) experiment [14]. Two coherent laser beams with λ = 632.8 nm were irradiated on the composite in the tilted geometry at an incident angle of $\theta = 30°$ and 60° with respect to the composite's normal axis. The intensity of s-polarized writing beams was 30 mW/cm^2. The recorded PR grating was read by a p-polarized counter-propagating beam. An attenuated reading beam with a very weak intensity of 0.1 mW/cm^2 was used.

The magnitude of the space charge field was measured using the method reported previously [19]. The basic scheme of this method can be summarized as follows: the chromophore group, which had previously been aligned along the external electric field, was reoriented by the newly formed E_{sc}. A change in the birefringence was induced by the reorientation and was closely associated with the E_{sc}. Using numerical analysis based on the oriented gas model and the index ellipsoid method, the magnitude of the E_{sc} can be determined from the birefringence change. Details on this method have been well described in Ref. [19].

In order to characterize the electro-optic behavior of a given chromophore, the standard two crossed polarizers setup was used. The polarization axes of the analyzer and polarizer were set to 45° and −45° with respect to the incident plane, respectively, and the composite was tilted by 30° from the propagation direction of the prove beam.

3. Results and discussion

Table 1 shows the electron affinity (EA) and molecular weight of photosensitizers used in this work. The EA was calculated by using VAMP-AM1 method in the material studio 4.1 program. All the photosensitizers were found to form a CT complex with PSX-Cz in the solid state. The absorption spectra of five composites are shown in Fig. 2. The five composites had very different absorption spectra even though they were doped with the same amount (weight%) of photosensitizer. As expected from numerous studies performed on CT complexes in solid [20], we observed a linear relationship between the EA of the photosensitizer and the photon energy (E_{CT}) of the CT transition as shown in the inset of Fig. 2. At 632.8 nm, in particular, the values of the absorption coefficient (α) for TeNFM, TNF, TNFM, TCNE, and TCNQ composites were 18.0, 20.5, 32.1, 35.7 and 39.5 cm^{-1}, respectively.

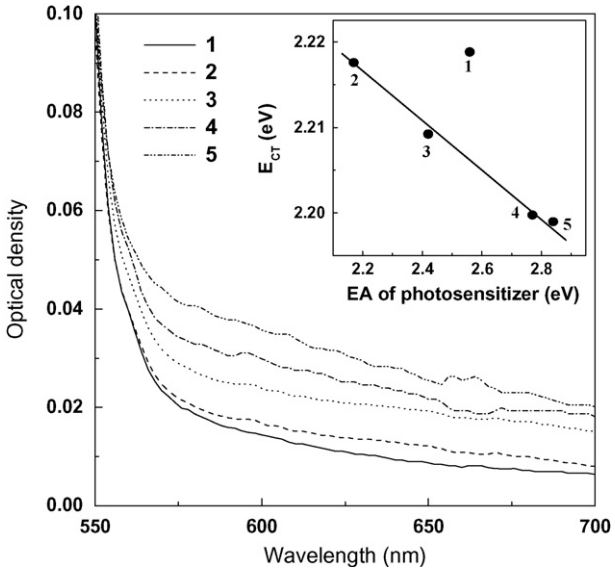

Fig. 2. Absorption spectra of five composites. The increased absorptivity in wavelength 550–700 nm is assigned to the charge-transfer complex between PXS-Cz and photosensitizer. Inset: Correlation between the photosensitizer electron affinity and the optical transition energy of the charge-transfer complex, formed between the PSX-Cz and photosensitizer. For the composite numbering see Table 1. The line is a guide to the eye.

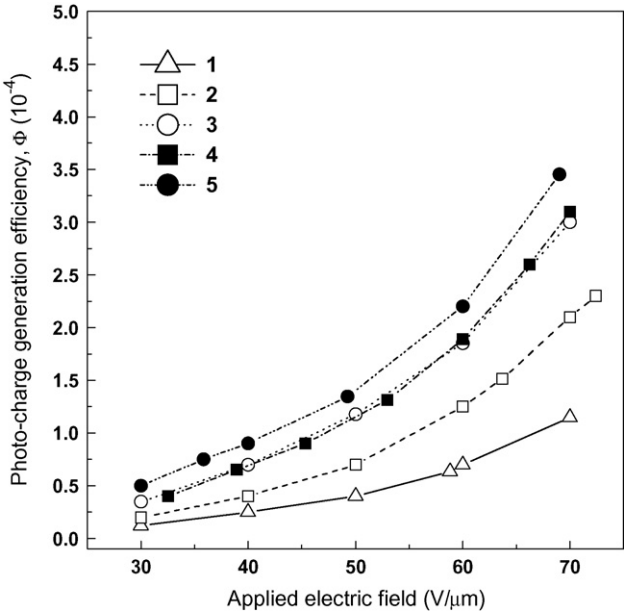

Fig. 3. Field dependence of the photo-charge generation efficiency for composite 1 (open triangles), 2 (open squares), 3 (open circles), 4 (closed squares), 5 (closed circles). The line is a guide to the eye.

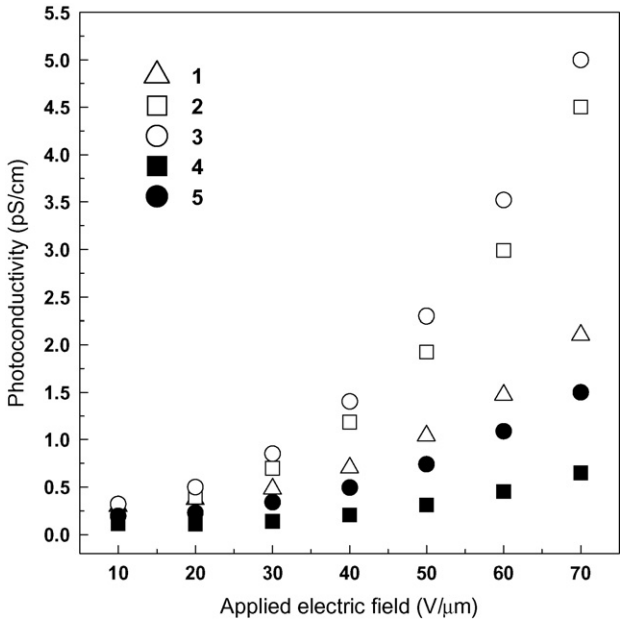

Fig. 5. Field dependence of the photoconductivity for composite 1 (open triangles), 2 (open squares), 3 (open circles), 4 (closed squares), 5 (closed circles).

The amount of available charges, which can be indicated as photo-charge generation efficiency (Φ), is the important parameter in the buildup of the space charge field in the PR composites [21]. We have studied the field dependence of the photo-charge generation efficiency of five composites. For clarity, we show the experimental data of five composites in Fig. 3. The photo-charge generation efficiency exhibited strong electric field dependence which can be simulated theoretically by Onsager's model of the geminate-pair dissociation. The photo-charge generation efficiency of five composites was in the following order: composite 1 < composite 2 < composite 3 < composite 4 < composite 5. As shown in Fig. 4, the photo-charge generation efficiency is directly proportional to the absorption coefficient [22]. For 5 composite doped TCNQ with a high electron affinity, larger amounts of the CT complex are formed; more charges are generated due to the increased absorption of incident writing light [23].

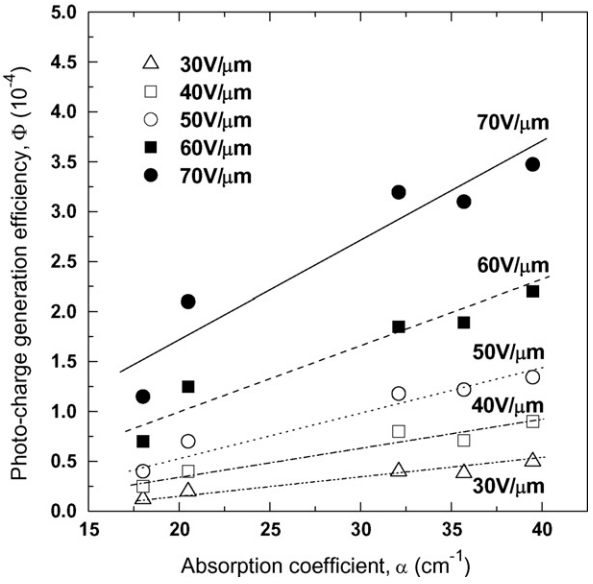

Fig. 4. The correlation between the photo-charge generation efficiency and the absorption coefficient at 632.8 nm for composites 1–5. The line is a guide to the eye.

Another important parameter in the buildup of the space charge field, next to the amount of available charges, is the trap density in the PR composites [21]. When the energy level of the photosensitizer LUMO is higher than that of the charge transporter HOMO, the photosensitizer anion, which is generated by excitation of the CT complex followed by electron transfer and the subsequent dissociation of the negatively charged photosensitizer and the oxidized charge-transport species in an electric field, will act as a trap in PR polymer composites. This has been investigated thoroughly by Grunnet-Jepsen et al. in PVK-based polymer composites containing C_{60} as a photosensitizer [24]. They found a good correlation between the spectroscopically determined concentration of C_{60}^- anions and the active trap density, calculated from PR measurements. In similar composites, the buildup of the PR effect was found to slow down if the composite had been preilluminated while applying a strong electric field [25]. This was attributed to the activation of deep trapping sites by optical illumination, known as optical trap activation [26]. Although less pronounced, and without spectroscopic evidence for the formation of photosensitizer anions, such as TeNFM$^-$, TNF$^-$, TNFM$^-$, TNCE$^-$, and TCNQ$^-$, we have observed similar effects in our five sensitized composites. The sensitizers act as efficient photosensitizers for PSX-Cz because the HOMO level is below that of PSX-Cz. When optical excitation of the HOMO-LUMO transition of sensitizer occurs, an electron in the HOMO of a nearby carbazole molecule can be transferred to sensitizer, producing sensitizer anion and a mobile hole in PSX-Cz [24]. And then, the sensitizer anions act as a trap for photogenerated holes. As shown in Fig. 5, the photoconductivities of composite 1–3 were increased with the photo-charge generation efficiency; however, the photoconductivities of composite 4 and 5 were found to decrease slightly, although they generated more charge compared to the other composites through the larger CT complex and light absorption. This is consistent with the formation of a larger amount of photosensitizer anion traps. Composite 4 and 5 doped with a larger number of photosensitizer molecules (Table 1) have a larger number of photosensitizer anion traps.

By our previously reported method [19], we have measured the space charge field of composites 1–5 as a function of the applied

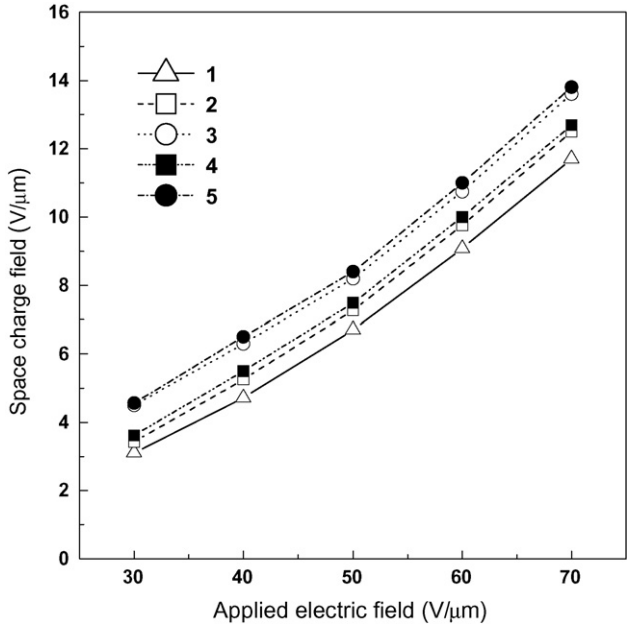

Fig. 6. Field dependence of the space charge field for composite 1 (open triangles), 2 (open squares), 3 (open circles), 4 (closed squares), 5 (closed circles). The line is a guide to the eye.

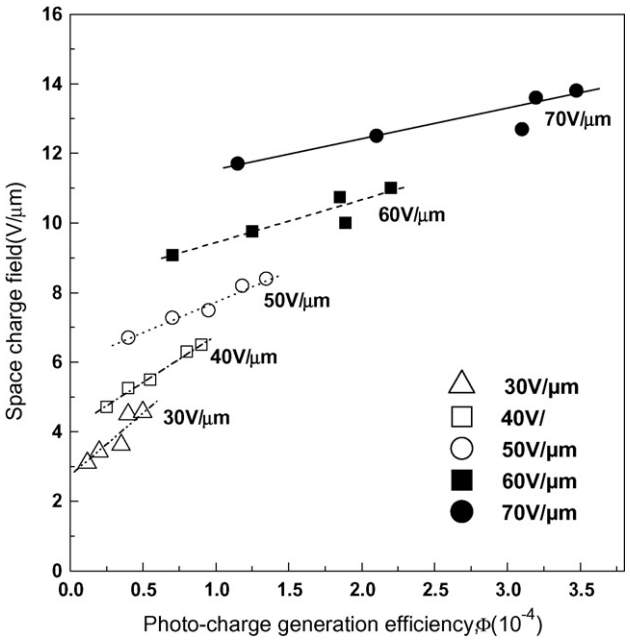

Fig. 7. Correlation between the space charge field and the photo-generation efficiency at 30–70 V/μm for composites 1–5. The line is a guide to the eye.

electric field. For clarity, Fig. 6 shows the experimental data of the composites. The E_{sc} increased linearly with an increasing electric field. The electric field dependence of the E_{sc} resulted from electric-field-assisted separation of charge from the electron–hole pair with a high energy distribution. The E_{sc} of five composites was in the following order: composite 1 < composite 2 < composite 4 < composite 3 < composite 5. According to Poisson's equation, the magnitude of the space charge field is changed with generated charge and trap density [27]. When electron–hole pairs are generated in the bright region, the holes are hopped to the neighbor transport sites by the externally applied electric field and then they are trapped in the dark region. After separation of electron and hole charges occurs, the E_{sc} is formed between bright and dark regions. Fig. 7 shows the dependence of the space charge field on the photo-charge generation efficiency. The E_{sc} increased with increasing photo-charge generation efficiency in the same external electric field. The composite with higher photo-charge generation efficiency, more charges are available to build up the E_{sc}. Note that larger E_{sc} can be sustained as the trap density as well as the charge density is increased. Together with the increasing amount of available charges, the larger trap density therefore explains the increasing tendency of the space charge field in composites 1–5. Particularly, composite 5 having the larger charge and trap density shows the larger E_{sc} amplitude than the other composite.

The steady-state diffraction efficiencies of composites 1–5 were measured as a function of the applied electric field. The experiments were carried out at $T_g + 3\,^{\circ}C$ to take full advantage of the birefringence contribution to the index modulation amplitude. The refractive index modulation amplitudes Δn were calculated using Kogelnik's expression for the internal diffraction efficiency (η) in thick transmission holograms [28],

$$\eta = \sin^2\left[\frac{\pi d\,\Delta n\,\cos(\theta_2 - \theta_1)}{\lambda\sqrt{\cos\theta_1\,\cos\theta_2}}\right] \quad (1)$$

where d is the composite thickness, λ is the wavelength, and θ_1 and θ_2 are the internal angle of incidence of the two writing beams. Fig. 8 shows the refractive index modulation of composites 1–5 as a function of the applied electric field. The refractive index modulation of five composites was in the following order: composite 1 < composite 2 < composite 4 < composite 3 < composite 5. The refractive index modulation directly increased with increasing magnitude of the E_{sc}. TCNQ composite having lager E_{sc} shows higher refractive index modulation than the other composites. When larger amounts of the CT complex are formed by the intermolecular interaction between the photoconducting polymer and the photosensitizer (Fig. 2), more charges are generated due to the increased absorption of incident writing light (Fig. 4). Hence, more charges are available to build up the space charge field, resulting in a larger E_{sc} amplitude (Fig. 7) and a larger corresponding refractive index modulation amplitude (Fig. 8).

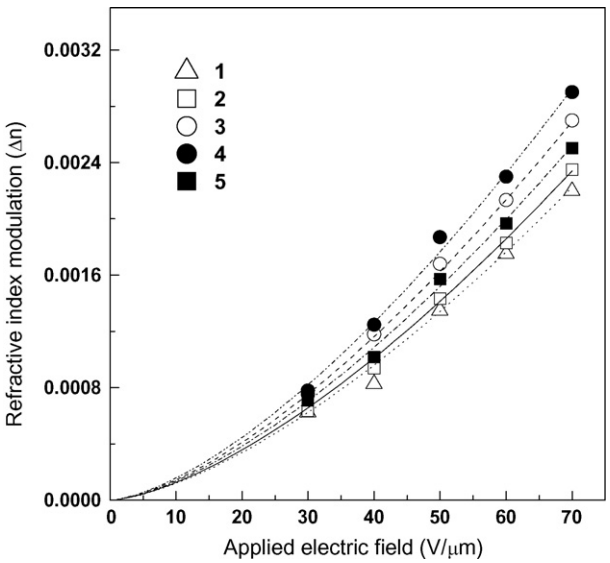

Fig. 8. Refractive index modulation amplitudes of composite 1 (open triangles), 2 (open squares), 3 (open circles), 4 (closed squares), 5 (closed circles) calculated from the internal diffraction efficiencies using Eq. (1), as a function of the applied electric field. The fits are according to $n = a \cdot E^b$ (see Ref. [24]).

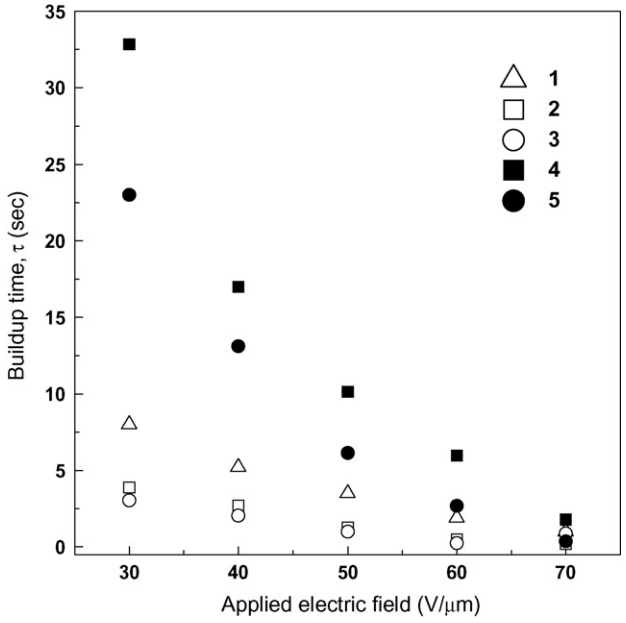

Fig. 9. Field dependence of the grating buildup time for composite 1 (open triangles), 2 (open squares), 3 (open circles), 4 (closed squares), 5 (closed circles).

The PR grating buildup rate and the photoconductivity for the five composites were also analyzed. PR grating buildup rate, which is very important for real applications such as a real-imaging and real-data processing, consists of (1) a buildup of a space charge field involving the photogeneration of charges and their redistribution and (2) modulation of the refractive index through an electro-optic effect. As a result, the grating buildup time of the low T_g PR composites is limited by the photoconductivity and the orientational mobility of the chromophore. In this study, among several factors that constitute PR composite, only photosensitizer was controlled. Therefore, the buildup time (τ) will be related to the photoconductivity of the material. The buildup time of the PR composites was evaluated from the buildup of the beam intensity of the DFWM measurement. The time constants, τ_1 and τ_2, were calculated by fitting the evolution of the growth of the gain, $g(t)$, with the following biexponential function [29],

$$g(t) = a_1 \left\{1 - \exp\left(-\frac{t}{\tau_1}\right)\right\} + a_2 \left\{1 - \exp\left(-\frac{t}{\tau_2}\right)\right\} \quad (2)$$

where τ_1 and τ_2 are the fast and slow time constants, respectively. Fig. 9 shows the τ_1 of composites 1–5, which were measured at five different electric fields between 30 and 70 V/μm. An elevated external electric field causes faster grating formation in all composites, as was expected, since the charge mobility as well as the photo-charge generation efficiency increase with electric field. In five composites, the PR grating buildup rate is increased with the photoconductivity. In composite 1–3, increasing the absorption coefficient leads to a larger photoconductivity, space charge field and a faster grating buildup through a faster photo-charge generation. Composite 4 and 5, however, have lower photoconductivity and smaller buildup rates due to reduction of hole mobility with the larger amount of traps produced by photoreduction of the photosensitizer.

4. Conclusions

In this work, we focused and discussed the sensitizer effect on the overall photorefractive performances, since it is important to examine the essential role of sensitizer for developing new photorefractive systems. We measured overall PR properties such as space charge field, refractive index modulation, and PR grating buildup time in five PR composites which were doped with various photosensitizers having each different electron affinity. The photon energy of the CT transition decreased with increasing electron affinity of the photosensitizer. In PR composites doped with TeNFM, TNF, and TNFM, the photoconductivity and the PR grating buildup rate increase as more charges are generated by increasing of absorption coefficient. The refractive index modulation is also enhanced as the absorption coefficient is increased, since more charges are available to build up the space charge field. However, in TCNE and TCNQ composites having a larger amount of photosensitizer anion traps, they have lower photoconductivity and PR grating buildup rate due to reduction of hole mobility by anion traps, although they generated more charge compared to the other composites. Further study on the relationship between photo-charge generation, transport, and trap will be required to clarify the photosensitizer effect on the photoconductivity and the PR grating buildup time.

Acknowledgements

This work was supported by the Korea Science and Engineering Foundation (KOSEF) grant funded by the Korea government (MEST) (Grant No. R11-2007-050-01003-0) and by the Research fund of HYU (HYU-2008-T).

References

[1] T. Tschudi, A. Herden, J. Goltz, H. Klumb, F. Laeri, J. Albers, IEEE J. Quantum Elect. QE-22 (8) (1986) 1493–1502.
[2] L.B. Aronson, L. Hesselink, Opt. Lett. 15 (1) (1990) 30–32.
[3] Y. Zhang, T. Wada, H. Sasabe, J. Mater. Chem. 8 (4) (1998) 809–828.
[4] O. Oksana, W.E. Moerner, Chem. Rev. 104 (2004) 3267–3314.
[5] M.P. Georges, V.S. Scauflaire, P.C. Lemaire, Trends Opt. Photon. 62 (2001) 63–69.
[6] A.A. Kamshilin, S. Liu, H. Tuovinen, V.V. Prokofiev, T. Jaaskelainen, Opt. Lett. 19 (12) (1994) 907–909.
[7] W.-J. Joo, N. Kim, Polym. J. (Tokyo JT Japan) 36 (9) (2004) 674–678.
[8] P. Yu, S. Balasubramanian, T.Z. Ward, M. Chandrasekhar, H.R. Chandrasekhar, Synth. Met. 155 (2) (2005) 406–409.
[9] J.A. Herlocker, L.B. Ferrio, E. Hendrickx, B.D. Guenther, S. Mery, B. Kippelen, N. Peyghambarian, Appl. Phys. Lett. 74 (1999) 2253–2255.
[10] J.S. Schildkraut, A.V. Buettner, J. Appl. Phys. 72 (1992) 1888–1893.
[11] E. Hendrickx, B. Kippelen, S. Thayumanavan, S.R. Marder, A. Persoons, N. Peyghambarian, J. Chem. Phys. 112 (21) (2000) 9557–9561.
[12] H. Bässler, Phys. Status Solidi B 175 (1993) 15–56.
[13] Y.P. Cui, B. Swedek, N. Cheng, J. Zieba, P.N. Prasad, J. Appl. Phys. 85 (1999) 38–43.
[14] H. Chun, I.K. Moon, D.H. Shin, N. Kim, Chem. Mater. 13 (2001) 2813–2817.
[15] J.C. Scott, L.Th. Pautmeier, W.E. Moerner, J. Opt. Soc. Am. B 9 (1992) 2059–2064.
[16] J. Mort, I. Chen, in: R. Wolfe (Ed.), Applied Solid State Science, vol. 5, Academic Press, New York, 1975, pp. 69–70.
[17] P.M. Borsenberger, D.S. Weiss, Organic Photoreceptors for Imaging Systems, Marcel Dekker Inc, New York, 1993, pp. 56–58.
[18] J.S. Schildkraut, Appl. Phys. Lett. 58 (1991) 340–342.
[19] W.-J. Joo, N.J. Kim, H. Chun, I.K. Moon, N. Kim, J. Appl. Phys. 91 (2002) 6471–6475.
[20] R. Foster, Organic Charge Transfer Complexes, Academic Press, London, 1969, pp. 40–43.
[21] D.V. Steenwinckel, E. Hendrickx, A. Persoons, J. Chem. Phys. 114 (21) (2001) 9557–9564.
[22] B.J. Mulder, Philips Res. Rept. Suppl. 4 (1968) 128–129.
[23] S.M. Silence, C.A. Walsh, J.C. Scott, W.E. Moerner, Appl. Phys. Lett. 61 (1992) 2967–2969.
[24] A. Grunnet-Jepsen, D. Wright, B. Smith, M.S. Bratcher, M.S. DeClue, J.S. Siegel, W.E. Moerner, Chem. Phys. Lett. 291 (1998) 553–561.
[25] E. Hendrickx, Y. Zhang, K.B. Ferrio, J.A. Herlocker, J.A. Anderson, N.R. Armstrong, E.A. Mash, A.P. Persoons, N. Peyghambarian, B. Kippelen, J. Mater. Chem. 9 (1999) 2251–2258.
[26] S.M. Silence, G.C. Bjorklund, W.E. Moerner, Opt. Lett. 19 (1994) 1822–1824.
[27] J.S. Schildkraut, A.V. Buettner, J. Appl. Phys. 72 (5) (1992) 1888–1893.
[28] H. Kogelnik, Bell Syst. Tech. J. 48 (1969) 2909–2912.
[29] M.A. Diaz-Garcia, D. Wright, B. Smith, E. Glazer, W.E. Moerner, Chem. Mater. 11 (1999) 1784–1791.